# Chapter 2

# Asymmetric Synthesis of Overcrowded Alkenes[1]
# Part I: Bisthioxanthylidenes

## 2.1 Introduction

Elaborate studies on sterically overcrowded alkenes have revealed their unique photochromic and dynamic properties (chapter 1).[2] Although lacking a stereogenic center, they may exist as stable, optically active stereoisomers due to the presence of substituents that cause steric hindrance between the upper and lower parts and enforce a helical distortion to the entire molecule. Unsymmetrical *cis* and *trans* isomers of overcrowded alkenes were shown to act as chiroptical molecular switches (section 1.2.6).[3] Current applications include the reversible transition between cholesteric and nematic phases when a liquid crystalline material is doped with optically active overcrowded alkenes[4], and the photochemical modification of chirality of thin polymer films modified with an optically active overcrowded alkene (section 1.2.8).[5] All these applications require optically active materials. Therefore a practical synthetic route toward enantiomerically pure overcrowded alkenes is a challenging goal.

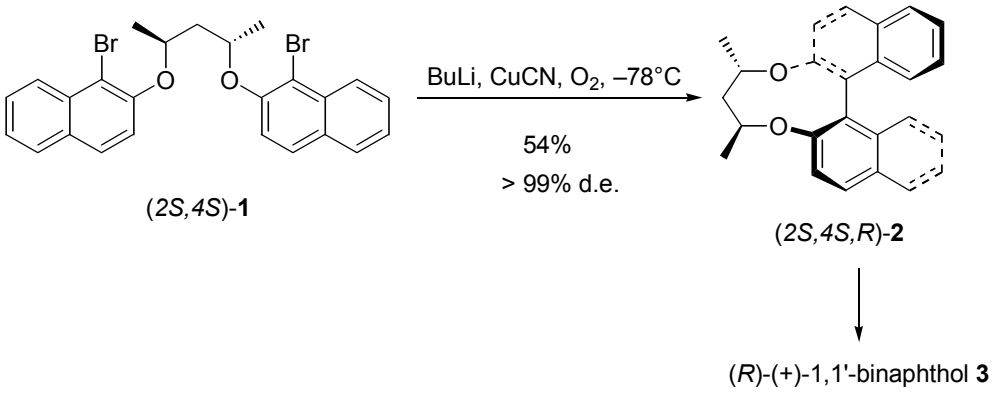


**Scheme 2.1** Synthesis of optical pure binaphthol **3** by axial single bond chirality control by employing optical pure 2,4-pentanediol as chiral template.

Methodology has been developed for the synthesis of optically active biaryls, in which control of axial single bond chirality is achieved by coupling of two aryl moieties to a chiral template.[6] The synthesis of optical pure binaphthol, reported by Sugimura et al., effected by axial single bond chirality control by optical pure 2,4-pentanediol, is a straightforward example (scheme 2.1).[7] Two 1-bromo-2-naphthol moieties were coupled to optical pure 2,4-pentanediol yielding (*2S,4S*)-**1**. A subsequent intramolecular coupling reaction resulted in formation of (*2S,4S,R*)-**2** as major product in

54% yield. The formation of the other possible stereoisomer (*2S,4S,S*)-**2** (not visualized) was not observed implying complete stereocontrol by the chiral template and a diastereomeric excess of >99%. Surprisingly, no intermolecularly coupled products were detected. Removal of the chiral bridge gave optical pure (*R*)-(+)-1,1'-binaphthol **3**.

Luh et al. succeeded to prepare optically active bifluorenylidenes along these lines (scheme 2.2).[8] (*S,S*)-threitol-ditosylate (*S,S*)-**4** served as a chiral template which was coupled with two fluorene moieties **5** to give pre-organized system **6**. The central double bond was constructed by intramolecular coupling upon treatment with tungsten hexacarbonyl. Thus optically active bisfluorenylidene (*S,S,P*)-**7** was obtained. Formation of the other possible diastereoisomer (*S,S,M*)-**7** was not observed. The absolute configuration of (*S,S,P*)-**7** was assigned after comparing its CD spectrum with that of related compounds. Removal of the chiral template resulted in the complete loss of optical activity of the bisfluorenylidene moiety as a result of a low Gibbs energy of activation ($\Delta G^{\ddagger}$) of the racemization process.

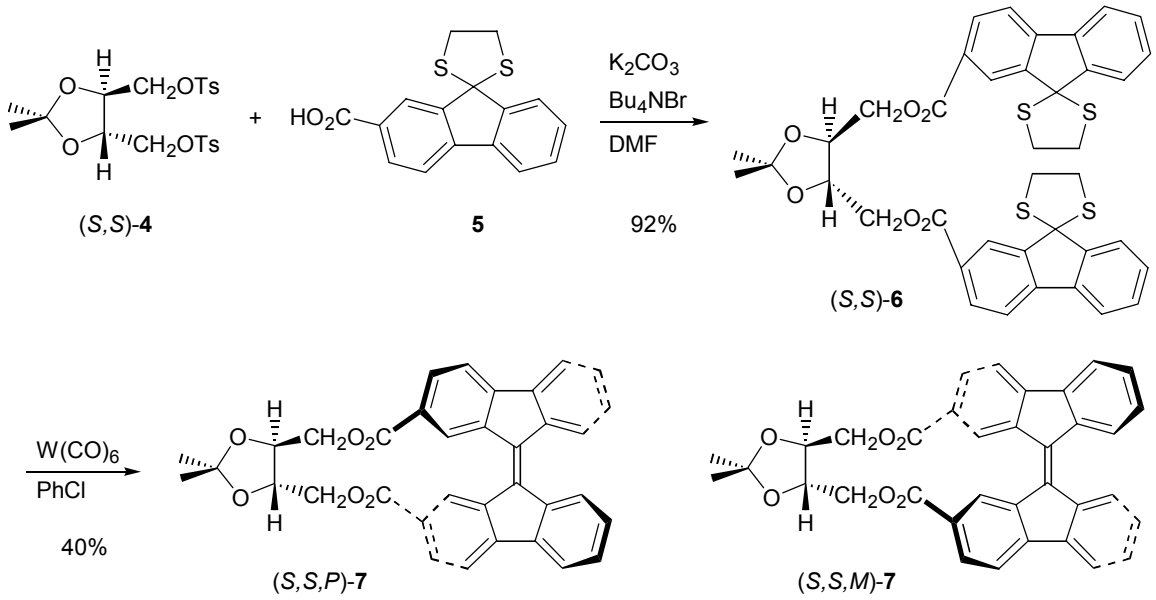


**Scheme 2.2** Synthetic route toward enantiomerically pure bisfluorenylidene (*S,S,P*)-**7**.

Based on the examples and methodology presented in schemes 2.1 and 2.2 we envisioned the synthesis of stable enantiomers of an overcrowded alkene which remain stable after removal of the chiral template (scheme 2.3). For this purpose we aimed for the synthesis of enantiomers of bisthioxanthylidene because of their relatively high Gibbs energy of racemization ($\Delta G^{\ddagger}_{rac.}$) of around 27.5 kcal $mol^{-1}$.[2i,9] This energy barrier implies that enantiomers of bisthioxanthylidene are sufficiently stable at room temperature and will not racemize fast after removal of the chiral template. First the upper and lower part, two thioxanthone moieties, of the overcrowded alkene are coupled to an enantiomerically pure chiral template. During a subsequent intramolecular coupling reaction the central double bond is constructed. The stereocontrol of the chiral template during the intramolecular coupling reaction should lead to enantiomerically pure bisthioxanthylidene after removal of the chiral template. (*S,S*)-Threitol-ditosylate-**4** (section 2.2), (*R*)-(+)-1,1'-binaphthol ((*R*)-**3**) and (*S*)-(–)-1,1'-

binaphthol ((*S*)-**6**) (section 2.3) were intended to be used as chiral templates. These two chiral templates feature axial singe bond chirality with the consequence that the sequence of events visualized in scheme 2.3 implies the realization of the intriguing concept of conveying axial single bond chirality to, stable, axial double bond chirality. We furthermore aimed for the first absolute configuration determination of enantiomerically pure bisthioxanthylidene. This was intended to be achieved by X-ray analysis of the intermediates formed after the intramolecular coupling reaction.

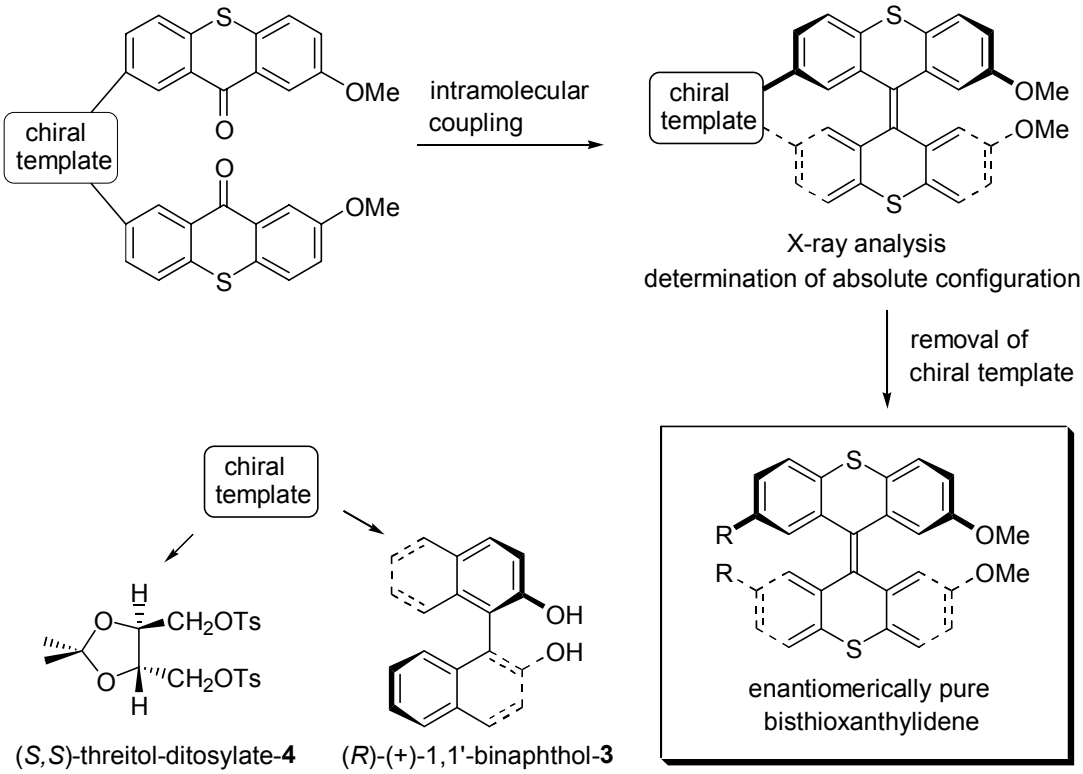


**Scheme 2.3** Synthetic approach toward enantiomerically pure bisthioxanthylidene.

## 2.2.1 Asymmetric Synthesis of Overcrowded Alkenes 13 with L-threitol Chiral Template

Initially we focussed on (*S,S*)-threitol-ditosylate (*S,S*)-**4** as chiral template. Two 7-methoxy-9-oxo-9*H*-thioxanthene-2-carboxylic acid moieties **11** were utilized as upper and lower part of the envisioned overcrowded alkene. Thioxanthone **11** was prepared from 4-methoxybenzenethiol **9** and 4-bromoisophthalic acid **8** in a two-step procedure (scheme 2.4). An aromatic substitution of thiol **9** and bromide **8** in refluxing DMF, under the influence of $K_2CO_3$ and Cu-bronze, furnished **10** in a 95% yield. Thioxanthone **11** was obtained in a 94% yield after an intramolecular Friedel-Crafts reaction induced upon treatment of **10** with thionyl chloride and $AlCl_3$, successively.

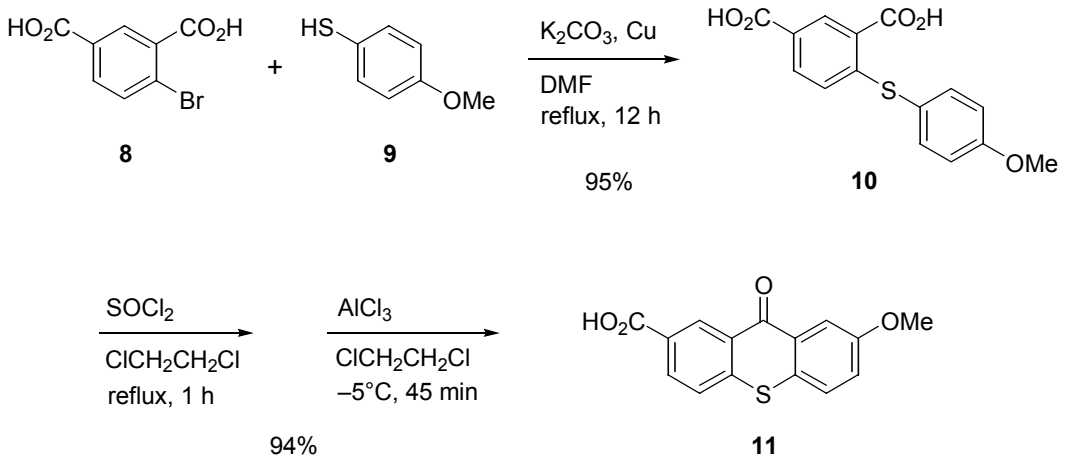


**Scheme 2.4** Two step preparation of thioxanthone **11**.

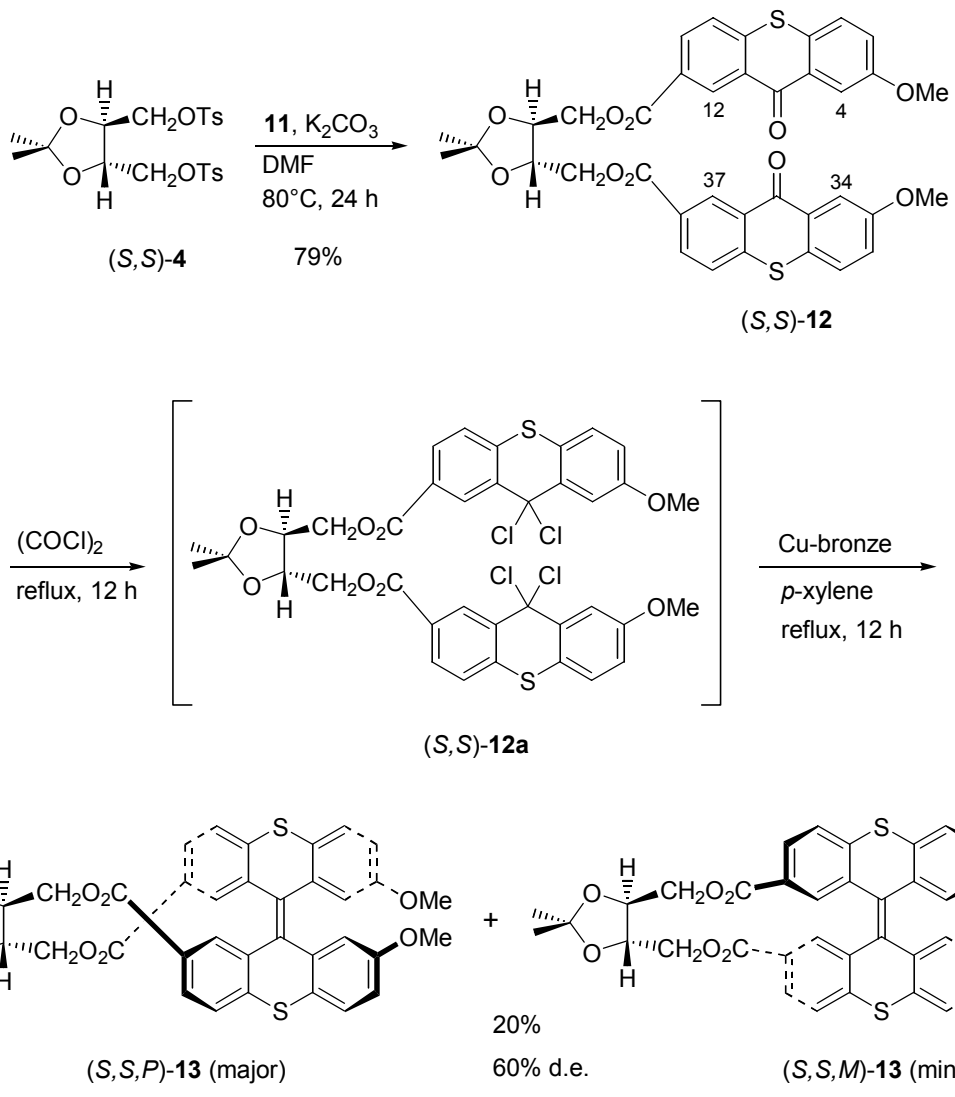


**Scheme 2.5** Synthetic route toward optically active overcrowded alkenes **13** using (*S,S*)-**4** as a chiral template.

Coupling of thioxanthone **11** to the threitol chiral template (*S,S*)-**4** resulted in formation of pre-

organized system (*S,S*)-**12** in a fair yield of 79% (scheme 2.5). (*S,S*)-**12** was subjected to an intramolecular copper-promoted *gem*-dichloride coupling reaction[10] affording the sterically overcrowded alkenes (*S,S,P*)-**13** (major product) and (*S,S,M*)-**13** (minor product) in 20% yield. Prior to this coupling reaction the two ketone moieties of (*S,S*)-**12** were converted into dichloride functionalities by the action of oxalyl dichloride. The thus created tetrachloride intermediate (*S,S*)-**12a** was not isolated and underwent *in situ* intramolecular coupling upon addition of Cu-bronze. The rather low yield of 20% was due to the extensive formation of oligomers as a result of intermolecular coupling reactions. This could not be suppressed by working at high dilution. A diastereomeric excess of 60% was determined by $^{1}$H NMR spectroscopy implying stereocontrol of the chiral template during the intramolecular coupling reaction which, however, was only moderate.

The chirality of the bridged overcrowded alkenes **13** is defined by (*S,S*), which denotes the configuration of the threitol moiety whereas (*P*) (right-handed helix) and (*M*) (left-handed helix) describe the helicity at the dimethoxy side of the overcrowded alkene part of the molecule (see section 1.1.4). The new overcrowded alkenes **13** were characterized by $^{1}$H and $^{13}$C NMR, high resolution spectrometry and X-ray analysis (section 2.2.2). Structural details are surveyed in section 2.2.3.

## 2.2.2 Determination of the Absolute Configuration of Alkenes 13

Recrystallization of **13** from acetone gave crystals of pure (*S,S,M*)-**13** (minor product) that were suitable for X-ray analysis (figure 2.1). From the analysis the absolute configuration of (*S,S,M*)-**13** (minor product) could be assigned. The unique folded structure of the overcrowded alkene part of (*S,S,M*)-**13** is clearly visible and based on the (*2S,3S*)-configuration of the threitol[14] moiety an (*M*)-configuration for the dimethoxy side of the overcrowded alkene was established. The helical structure of (*S,S,M*)-**13** (minor) is quantified by torsion angles of 50.6 [C(1)-C(2)-C(11)-C(12)] and 3.9 degrees [C(36)-C(1)-C(2)-C(11)], respectively. Assignment of atom numbers proceeded according to IUPAC nomenclature. Scheme 2.6 shows the complete atom numbering of (*S,S,M*)-**13** (minor) and (*S,S,P*)-**13** (major). Despite several attempts the major isomer (*S,S,P*)-**13** could not be obtained diastereomerically pure.

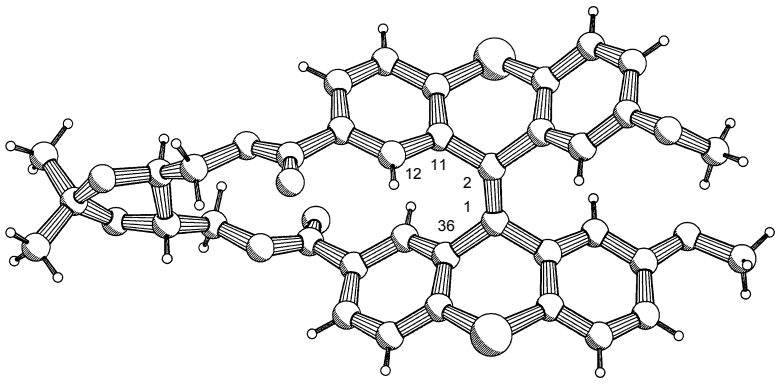


**Figure 2.1** PLUTON representation of structure (*S,S,M*)-**13** (minor).

## 2.2.3 Structural Features

The formation of overcrowded alkenes **13** was confirmed by the chemical shift of protons $H_{12,37}$ and $H_{4,34}$ which are situated in the fjord region of the molecules (scheme 2.6). Protons in this region of overcrowded alkenes characteristically exhibit chemical shifts at high field due to anisotropic shielding effects. Indeed, chemical shifts of protons $H_{12,37}$ and $H_{4,34}$ considerably shifted to higher field when compared with the chemical shift they exhibited in (*S,S*)-**12** (table 2.1).

**Table 2.1** Chemical shifts of protons $H_{12,37}$ and $H_{4,34}$ in (*S,S*)-**12** and overcrowded alkenes **13**.

| | (*S,S*)-**12** | (*S,S,M*)-**13** (minor) | (*S,S,P*)-**13** (major) |
|---|---|---|---|
| δ $H_{12,37}$ (ppm) | 9.12 | 7.08 | 7.03 |
| δ $H_{4,34}$ (ppm) | 7.93 | 6.35 | 6.38 |

Numbering of protons $H_{12,37}$ and $H_{4,34}$ according IUPAC nomenclature for diastereoisomers **13**. According to these rules, the comparable protons in (*S,S*)-**12** (scheme 2.6) have other numbers, but for the sake of clarity we have used the same numbering scheme of **13** for (*S,S*)-**12** here.

As visualized in schemes 2.5 and 2.6, the two diastereoisomers (*S,S,M*)-**13** (minor) and (*S,S,P*)-**13** (major) significantly differ in molecular shape. X-Ray analysis of (*S,S,M*)-**13** (minor) revealed a 'linear' coupling of the chiral threitol template with the overcrowded alkene part. The structural differences with its 'crossed' coupled (*S,S,P*)-**13** (major) isomer are confirmed by differences in chemical shifts ($^1$H NMR) of protons in the vicinity of the ester bonds (table 2.2). Though diastereoisomer (*S,S,P*)-**13** (major) was not obtained completely pure, chemical shifts of all protons were assigned in a $^1$H NMR spectrum of a mixture of both diastereoisomers.

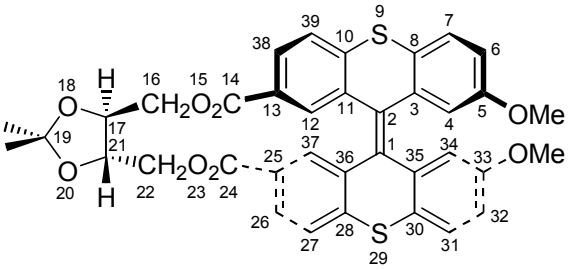


(*S,S,M*)-**13** (minor)
'linearly' coupled

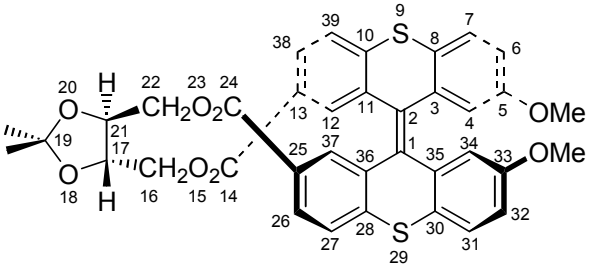


(*S,S,P*)-**13** (major)
'crossed' coupled

**Scheme 2.6** 'Linearly' coupled product (*S,S,M*)-**13** (minor) and 'crossed' coupled product (*S,S,P*)-**13** (major). Numbering of atoms according IUPAC nomenclature.

**Table 2.2** Chemical shifts (δ) of protons $H_{17,21}$ and $H_{16,22}$.

| | $H_{17,21}$ | $H_{16,22,eq}$ | $H_{16,22,ax}$ |
|---|---|---|---|
| (*S,S,M*)-**13** (minor) | 3.98 | 4.17 | 4.29 |
| (*S,S,P*)-**13** (major) | 4.29 | 4.80 | 4.02 |

Differences of 0.27 to 0.63 ppm were observed for protons in the ester bond region and, remarkably, the observed differences between corresponding aromatic protons of both diastereoisomers were 0.05 ppm at most. Apparently, the shape and chemical environment of the overcrowded alkene part of both diastereoisomers are practically identical.

## 2.3 Asymmetric Synthesis of Overcrowded Alkenes 16 with 1,1'-Binaphthol Chiral Template

In order to increase the yield of the intramolecular coupling reaction we embarked on the employment of chiral templates (*R*)-(+)-1,1'-binaphthol (*R*)-**3** and (*S*)-(–)-1,1'-binaphthol (*S*)-**3** [scheme 2.7 depicts the route to (*R*)-**3**, the same procedure was applied for (*S*)-**3**]. The rigidity of these templates, compared to template (*S,S*)-**4**, was supposed to enhance intramolecular coupling and to diminish intermolecular coupling.

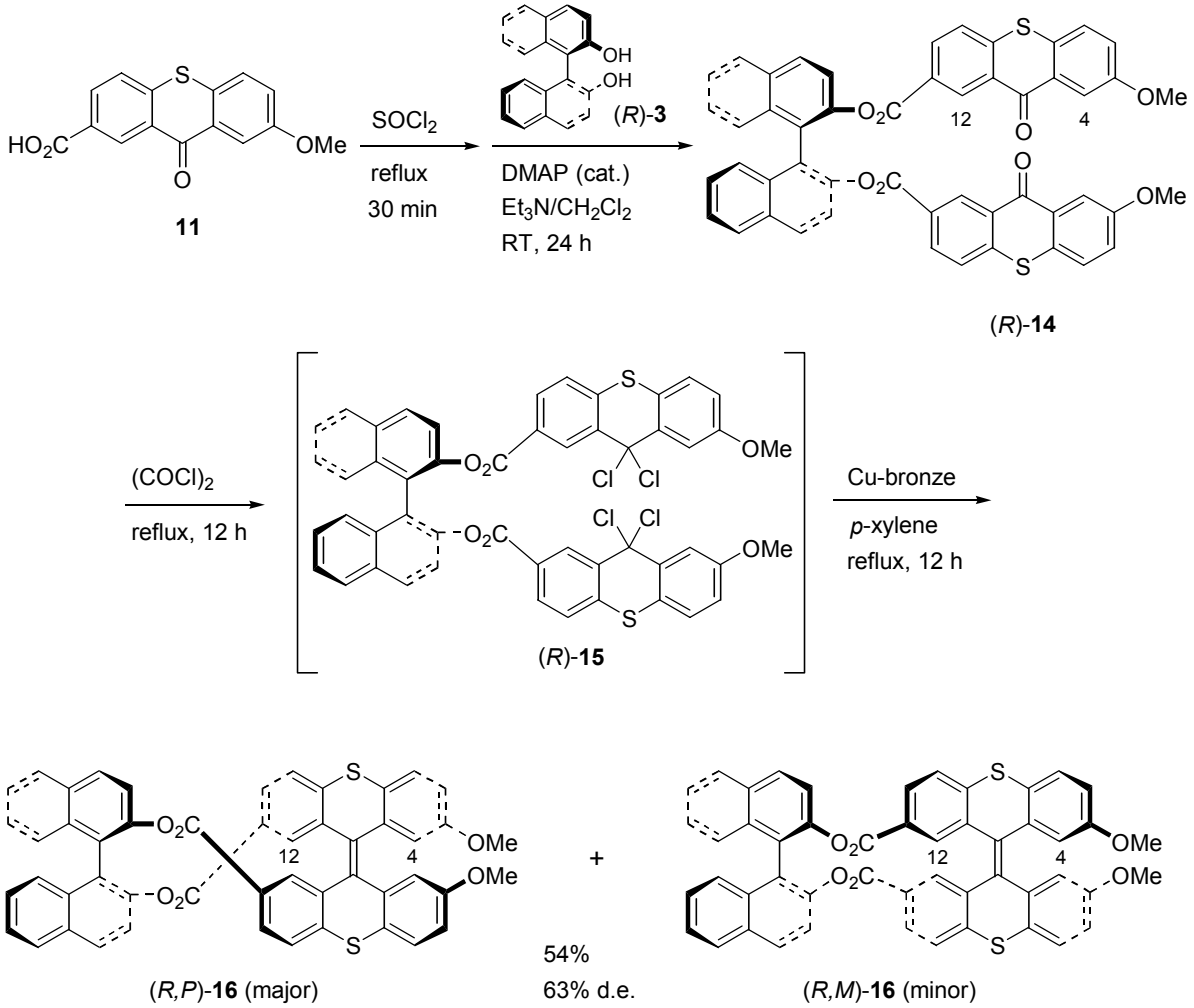


**Scheme 2.7** Synthetic route toward optically active overcrowded alkenes **16** with (*R*)-**3** as chiral template.

Diester (*R*)-**14** was prepared from thioxanthone **11** and (*R*)-(+)-1,1'-binaphthol (*R*)-**3** in two steps in a nearly quantitative yield. More importantly, the yield of the subsequent intramolecular *gem*-dichloride coupling reaction, with oxalyl dichloride and Cu-bronze, increased considerably with respect to the 20% yield of the overcrowded alkenes **13** described in section 2.2. Diastereoisomers (*R,P*)-**16** (major) and (*R,M*)-**16** (minor) were obtained in a yield of 54%. An 81.5/18.5 ratio of diastereoisomers (*R,P*)-**16** (major) and (*R,M*)-**16** (minor) was established by $^1$H NMR. As anticipated the rigidity of the binaphthyl template enforced a favorable orientation of the two thioxanthene moieties of tetrachloride (*R*)-**15** for intramolecular coupling. Apart from alkenes **16** only starting material was recovered after reaction implying no intermolecular coupling took place.

Although the geometry of (*R*)-**15** enhanced selectivity of intramolecular *versus* intermolecular coupling, the stereocontrol of the binaphthol (63% d.e.) and L-threitol templates (60% d.e., section 2.2) were nearly identical. Diastereoisomers (*R,P*)-**16** (major) and (*R,M*)-**16** (minor) were readily separated by column chromatography and have been fully characterized. The chirality of overcrowded alkenes **16** is defined by (*R*) and (*S*) for the configuration of the binaphthol moiety and (*P*) (right-handed helix) and (*M*) (left-handed helix) for the helicity at the dimethoxy side of the overcrowded alkene part of the molecule (compare section 1.1.4).

Analogous to overcrowded alkenes **13**, the chemical shift of protons $H_4$ and $H_{12}$ (scheme 2.7) of diastereoisomers (*R,M*)-**16** (minor) and (*R,P*)-**16** (major), which are situated in the fjord region, were found at high field (table 2.3). An upfield shift of at least 1.5 ppm was found as compared to the pre-organized system (*R*)-**14**.

**Table 2.3** Chemical shifts of protons $H_4$ and $H_{12}$ in (*R*)-**14** and overcrowded alkenes **16**.

| | (*R*)-**14** | (*R,M*)-**16** (minor) | (*R,P*)-**16** (major) |
|---|---|---|---|
| $\delta$ $H_4$ (ppm) | 8.01 | 6.39 | 6.36 |
| $\delta$ $H_{12}$ (ppm) | 9.02 | 7.54 | 7.31 |

Numbering of protons $H_4$ and $H_{12}$ according to IUPAC nomenclature for diastereoisomers **16**. Note that the comparable protons in (*R*)-**14** have been given the same numbers for the sake of comparison.

The absolute configurations of the two different diastereoisomers, (*R,P*)-**16** (major) and (*R,M*)-**16** (minor), were determined after cleavage of the binaphthol templates (section 2.4). The configuration of the overcrowded alkene parts were assigned by comparison, with data such as 1) order of elution by chiral HPLC, 2) CD, and 3) optical rotation, with the overcrowded alkene part originating from (*S,S,M*)-**13** (minor), of which the absolute configuration was established by X-ray analysis (section 2.2). It should be emphasized that both a folded and twisted structural moiety is present in molecules (*R,P*)-**16** (major) and (*R,M*)-**16** (minor). The two diastereoisomers differ significantly in structure as is visualized in schemes 2.7 and 2.8. Although in both isomers the binaphthyl part is twisted and the thioxanthylidene is folded, the formation of the 'crossed' coupled product (*R,P*)-**16** (major) is strongly favored over the 'linearly' coupled product (*R,M*)-**16** (minor). Figure 2.2 shows an optimized space filling model of (*R,P*)-**16** (major)[12] revealing an appealing double helix type structure which is

reminiscent of the helical structure found by Nozaki et al. for their double-helical oligo esters.[11]

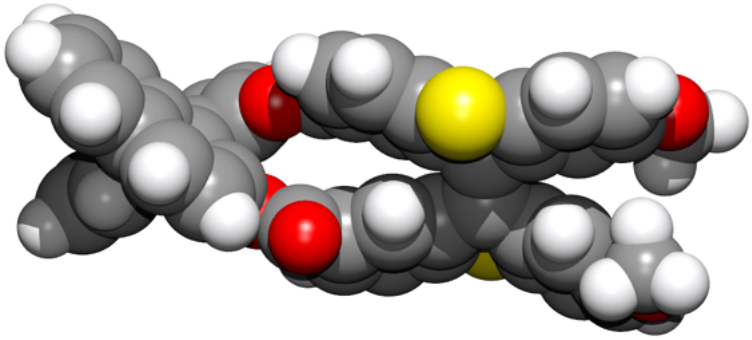

**Figure 2.2** A model of (*R,P*)-**16** (major) optimized with a CHARMm 23 force field as implemented in Quanta97/CHARMm.[12] The structure is viewed along the binaphthol single bond and the alkene double bond.

Diastereoisomers (*R,P*)-**16** (major) and (*R,M*)-**16** (minor) were characterized by exact mass and $^{1}H$, $^{13}C$, COSY, and NOESY NMR spectroscopy. By means of COSY and NOESY NMR all 12 different proton signals of both diastereoisomers could be assigned unequivocally. The structural difference between both diastereoisomers, particularly in the vicinity of the ester bonds, was confirmed by variation in chemical shifts of protons $H_{12}$, $H_{17}$, and $H_{51}$ (scheme 2.8 and table 2.4). See experimental section for the complete atom numbering scheme of (*R,M*)-**16** (minor) and (*R,M*)-**16** (major).

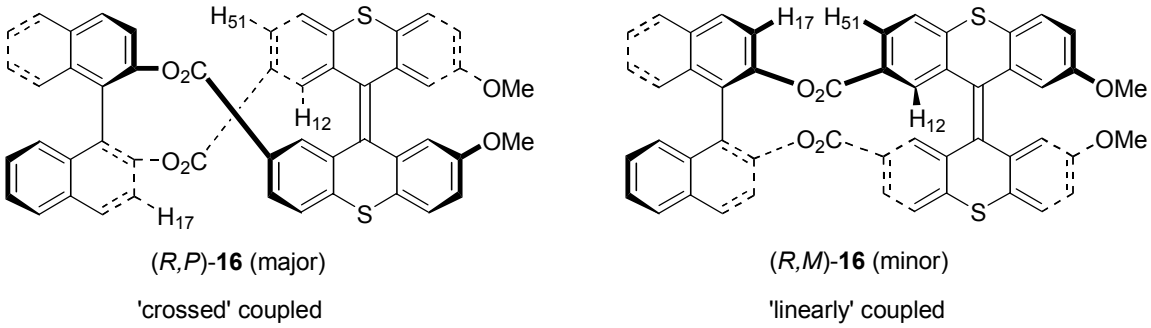


**Scheme 2.8** 'Crossed' coupled product, (*R,P*)-**16** (major) and 'linearly' coupled product (*R,M*)-**16** (minor).

**Table 2.4** Chemical shifts (δ) of protons $H_{12}$, $H_{17}$, and $H_{51}$.

| | $H_{12}$ | $H_{17}$ | $H_{51}$ |
|---|---|---|---|
| (*R,P*)-**16** (major) | 7.31 | 7.25 | 7.01 |
| (*R,M*)-**16** (minor) | 7.54 | 7.39 | 7.39 |

Protons $H_{12}$, $H_{17}$, and $H_{51}$ of the minor isomer (*R,M*)-**16** appear at lower field with respect to protons $H_{12}$, $H_{17}$, and $H_{51}$ of the major isomer (*R,P*)-**16**: $\Delta\delta$ ($H_{12}$) = 0.23 ppm, $\Delta\delta$ ($H_{17}$) = 0.14 ppm, and $\Delta\delta$ ($H_{51}$) = 0.38. All other corresponding protons of the two isomers do not differ significantly with $\Delta\delta$ not exceeding 0.09 ppm.

## 2.4 Synthesis of Enantiomerically Pure Bisthioxanthylidene 17 by Removal of Chiral Templates

The overcrowded alkenes (*S,S,M*)-**13** (minor), (*R,P*)-**16** (major), (*R,M*)-**16** (minor), (*S,M*)-**16** (major), and (*S,P*)-**16** (minor) were liberated from their chiral template by reduction with $LiAlH_4$ which provided enantiomers of bisthioxanthylidenes (*P*)-*cis*-**17** and (*M*)-*cis*-**17** with e.e. values of 96% ± 1% as was determined by chiral HPLC (scheme 2.9). Portions of binaphthol, recovered from the reaction mixtures, were found to have similar e.e. values (chiral HPLC). Since the commercially binaphthol **3** used in these reactions initially had an e.e. of 99%, the series of reactions, most probably the Cu-bronze promoted coupling step, caused a decrease in e.e. of only 3%.

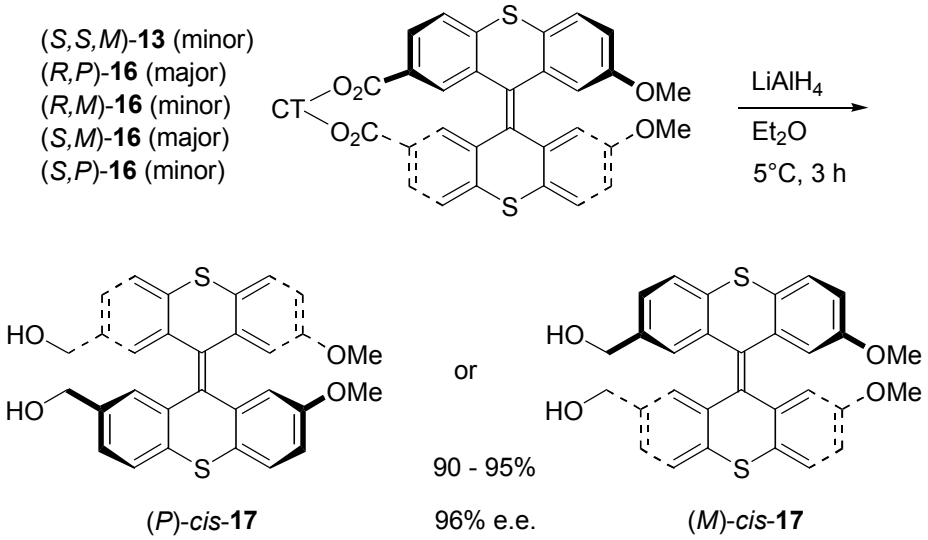


**Scheme 2.9** Cleavage from the chiral templates (CT) from overcrowded alkenes **13** and **16**. (*P*) (right-handed helix) and (*M*) (left-handed helix) define the helicity at the dimethoxy side of *cis*-**17**.

**Table 2.5** Stereochemical correlation and optical rotation data of **13**, **16**, and **17**.

| substrate | $[\alpha]_D^{20}$[a] | product | $[\alpha]_D^{20}$[a] |
|---|---|---|---|
| (*S,S,M*)-**13** (minor) | +203[b] | (*M*)-*cis*-**17** | –92 |
| (*R,P*)-**16** (major) | –101 | (*P*)-*cis*-**17** | +91 |
| (*R,M*)-**16** (minor) | +120 | (*M*)-*cis*-**17** | –93 |
| (*S,M*)-**16** (major) | +100 | (*M*)-*cis*-**17** | –92 |
| (*S,P*)-**16** (minor) | –120 | (*P*)-*cis*-**17** | +91 |

[a] c = 1.00, $CHCl_3$, [b] c = 0.50, $CHCl_3$.

Based on the X-ray analysis of (*S,S,M*)-**13** (minor)(section 2.2) the overcrowded alkene part of (*S,S,M*)-**13** (minor) has an (*M*)-configuration leading to (*M*)-*cis*-**17** after removal of the L-threitol moiety. The analytical data of (*M*)-*cis*-**17** (optical rotation, CD data, and retention times on chiral HPLC) obtained from (*S,S,M*)-**13** (minor) were correlated with data of the enantiomers of *cis*-**17** obtained from diastereoisomers (*R,P*)-**16** (major), (*R,M*)-**16** (minor), (*S,M*)-**16** (major), and (*S,P*)-**16**

(minor). Results are outlined in table 2.5. A racemization barrier for *cis*-**17** of 26.7 ± 0.5 kcal mol$^{-1}$ ($\Delta G^{\ddagger}_{rac.}$, polarimetry at 70°C) was determined, in accordance with the observation that the enantiomers of *cis*-**17** are stable at room temperature.

## 2.5 UV and CD Measurements of Compounds 13, 16, and 17

**Table 2.6** UV spectra of compounds **13**, **16**, and **17**, recorded in *n*-hexane/*i*-propanol 80/20.

| compound | λ (nm) | ε (1000 cm$^2$ mol$^{-1}$) | | |
|---|---|---|---|---|
| (*S,S,M*)-**13** (minor) | 205 (77900) | * | 311 (17000) | * |
| (*R,P*)-**16** (major) | 224 (125000) | 278 (25600) | 306 (21400) | * |
| (*R,M*)-**16** (minor) | 222 (148600) | 286 (30400) | * | 378 (7100) |
| (*P*)-*cis*-**17** | 214 (67000) | 272 (15800) | * | 372 (6200) |

The four different UV spectra, outlined in table 2.6, show strong resemblance. Maxima were observed in four regions; 205 – 224 nm, 272 – 286 nm, 306 – 311 nm, and 372 – 378 nm, respectively. In case no absolute maximum was found, a shoulder was observed, marked with a *. These findings led us to conclude that the shape of these four UV-spectra are, to a large extent, determined by the nature of the overcrowded alkene part of the molecule and to a lesser extent by the shape of the entire molecule or the nature of the chiral template.

A pair of identical CD spectra (except for the sign) were obtained from enantiomers (*P*)-*cis*-**17** and (*M*)-*cis*-**17**. Seven maxima were observed at λ >215 nm for (*P*)-*cis*-**17** en (*M*)-*cis*-**17** (table 2.7). The CD absorptions as well as the Δε values are in good agreement with those obtained for related optically pure overcrowded alkenes which were previously obtained by preparative chiral HPLC.[13]

**Table 2.7** CD spectra of compounds **13**, **16**, and **17**, recorded in *n*-hexane/*i*-propanol 80/20.

| compound | λ (nm) | Δε (1000 cm$^2$ mol$^{-1}$) | | |
|---|---|---|---|---|
| (*S,S,M*)-**13** (minor) | 221 (–44.2) | 250 (+17.7) | 273 (–6.2) | 304 (+15.7) |
| | 341 (–2.4) | 390 (+1.6) | | |
| (*S,M*)-**16** (major) | 224 (+110.9) | 234 (–39.3) | 242 (+8.9) | 257 (–33.2) |
| | | 293 (+6.6) | 313 (–24.7) | |
| (*R,M*)-**16** (minor) | 225 (–264.0) | 236 (+86.3) | | 251 (–37.9) |
| | 276 (+3.7) | 293 (–24.9) | 318 (+41.1) | |
| (*P*)-*cis*-**17** | 220 (+37.9) | 229 (–17.6) | 239 (+11.6) | 252 (–18.0) |
| | 270 (+22.6) | 291 (–46.8) | 313 (+17.5) | |

Comparison of the four CD spectra of table 2.7 did not reveal a general tendency in terms of curve and sign. Although maxima and minima of (*S,M*)-**16** (major), (*R,M*)-**16** (minor), and (*P*)-*cis*-**17** emerge in same regions of the spectrum, no further similarities could be detected. Especially comparison of the CD spectra of the two diastereoisomers (*S,M*)-**16** (major) and (*R,M*)-**16** (minor) is

interesting (figure 2.3). The configuration of the overcrowded alkene parts is identical and the configuration of the binaphthol moieties are opposite. However, the CD curves are more or less mirror images of each other, except in the region of 240 to 280 nm. This implies that, in contrast with the above discussed UV spectra, no distinct structural feature is solely governing shape, sign, and intensity of the CD spectra but that the entire architecture of the two diastereoisomers (*S,M*)-**16** (major) and (*R,M*)-**16** (minor) is responsible.

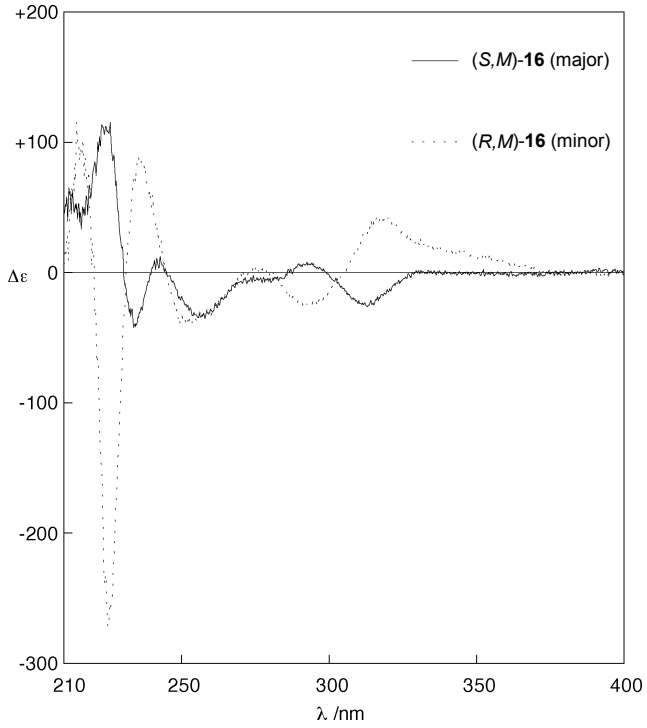


**Figure 2.3** CD spectra of diastereoisomers (*S,M*)-**16** (major) and (*R,M*)-**16** (minor).

## 2.6 Conclusions

The synthesis of stable enantiomers of 2,2'-dihydroxymethyl-7,7'-dimethoxy-bisthioxanthylidene **17**, featuring axial double bond chirality, was realized by using chiral templates [(*S,S*)-threitol-1,4-ditosylate ((*S,S*)-**4**), (*R*)-(+)-1,1'-binaphthol ((*R*)-**3**), and (*S*)-(–)-1,1'-binaphthol ((*S*)-**3**)]. In the most successful approach, two halves of the envisioned alkene were first coupled to a binaphthol chiral template after which a diastereoselective intramolecular coupling reaction afforded the corresponding overcrowded alkenes. After column chromatography and removal of the chiral template, both enantiomers of bisthioxanthylidene **17** were obtained separately with e.e.'s of 96%.

The binaphthol chiral templates feature axial single bond chirality with the consequence that, as no racemization of **17** was observed after removal of the chiral template, this sequence implies the realization of conveying axial single bond chirality to stable axial double bond chirality.

The employment of threitol (*S,S*)-**4** as chiral template provided a less attractive route to **17**, with

respect to reaction yields and purification. However, intermediate (*S,S,M*)-**13** (minor) was crystallized to allow determination of the absolute configuration of enantiomerically pure of 2,2'-dihydroxymethyl-7,7'-dimethoxy-bisthioxanthylidene ((*P*)-*cis*-**17**) by X-ray analysis.

## 2.7 Experimental Section

General: Melting points (uncorrected) were determined on a Mettler FP-2 melting point apparatus, equipped with a Mettler FP-21 microscope. $^{1}$H NMR spectra were recorded on a Varian Gemini-200 (200 MHz), a Varian VXR-300 (300 MHz), or a Varian Unity Plus Varian-500 (500 MHz). $^{13}$C NMR spectra were recorded on a Varian Gemini-200 (50 MHz), a Varian VXR-300 (75 MHz), or a Varian Unity Plus Varian-500 (125 MHz). Chemical shifts are denoted in δ-unit (ppm) relative to $CDCl_3$ (7.24), DMSO-$d_6$ (2.56), acetone-$d_6$ (2.19), benzene-$d_6$ (7.15), toluene-$d_8$ (2.09). The splitting patterns are designated as follows: s (singlet); d (doublet); t (triplet); q (quartet); m (multiplet) and br (broad). UV spectra were recorded on a Hewlett Packard HP 8453 UV-VIS spectrophotometer. CD spectra were recorded on a JASCO J-715 spectropolarimeter. MS spectra were obtained with a Jeol JMS-600 spectrometer by the electron ionization (EI) procedure. Column chromatography was performed on silica gel (Aldrich 60, 230-400 mesh) or on $Al_2O_3$ (neutral). The solvents were distilled and dried, if necessary, by standard methods. Reagents and starting materials were used as obtained from Aldrich and Syncom.

Specific for chapter 2: compound (*S,S*)-**4** was synthesized according to a literature procedure.[14]

**4-((4-Methoxyphenyl)sulfanyl)isophthalic acid (10)** Under a nitrogen atmosphere, 4-bromoisophthalic acid (**8**, 26.99 g, 110.16 mmol), 4-methoxybenzenethiol (**9**, 15.50 g, 110.56 mmol), Cu-bronze (250 mg, 3.93 mmol), and $K_2CO_3$ (38.00 g, 274.94 mmol) were refluxed overnight in DMF (500 mL). After cooling, the mixture was filtered and the residue was dissolved in water (250 mL). The solution was carefully acidified with concentrated HCl (aq.) to pH <1. The product precipitated and was collected on a glass filter. The product was thoroughly washed with water, dried at 100°C in air to yield pure **10** (31.80 g, 104.50 mmol, 95%) as a light pink powder. $^{1}$H NMR (200 MHz, DMSO-$d_6$, 25°C) δ 13.18 (br, 2H), 8.46 (d, $J$ = 1.8 Hz, 1H), 7.81 (dd, $J$ = 8.4, 1.8 Hz, 1H), 7.48 (d, $J$ = 8.8 Hz, 2H), 7.07 (d, $J$ = 8.8 Hz, 2H), 6.72 (d, $J$ = 8.4 Hz, 1H), 3.80 (s, 3H); $^{13}$C NMR (50 MHz, DMSO-$d_6$, 25°C) δ 166.66, 166.31, 160.60, 149.61, 137.42, 132.50, 131.93, 126.46, 126.16, 125.95, 120.97, 115.87, 55.31; HRMS calcd for $C_{15}H_{12}O_5S$: 304.041; found: 304.041.

**7-Methoxy-9-oxo-9*H*-thioxanthene-2-carboxylic acid (11)** Substrate **10** (31.80 g, 104.56 mmol) was refluxed in dichloroethane (300 mL) and $SOCl_2$ (65 mL) till HCl formation stopped (approximately 1 h). The mixture was concentrated *in vacuo* and the residue was stripped twice with dichloroethane. The residue was dissolved in dichloroethane (250 mL) and cooled to –5°C after which $AlCl_3$ (50.0 g, 375.0 mmol) of was added carefully. The resulting black mixture was stirred for 45 min at –5°C. The reaction was quenched by addition of 1.5 M HCl (aq.). The product was dissolved in $CH_2Cl_2$ (approximately 4 L). The organic layer was thoroughly washed with water (6 × 750 mL), dried ($Na_2SO_4$), and concentrated *in vacuo* to yield pure **11** (28.06 g, 98.11 mmol, 94%) as a yellow powder. $^{1}$H NMR (200 MHz, DMSO-$d_6$, 25°C) δ 8.98 (d, $J$ = 2.0 Hz, 1H), 8.18 (dd, $J$ = 8.4, 2.0 Hz, 1H), 7.94 (d, $J$ = 8.4 Hz, 1H), 7.93 (d, $J$ = 2.8 Hz, 1H), 7.83 (d, $J$ = 9.0 Hz, 1H), 7.45 (dd, $J$ = 9.0, 2.8 Hz, 1H), 3.89 (s, 3H); $^{13}$C NMR (50 MHz, DMSO-$d_6$, 25°C) δ 178.39, 166.67, 158.72, 141.71, 132.26, 130.58, 129.62, 128.92, 128.48, 127.95, 127.69, 127.33, 122.97, 110.61, 55.76; HRMS calcd for $C_{15}H_{10}O_4S$: 286.030; found: 286.028.

**(*S,S*)-(5-((((7-Methoxy-9-oxo-9*H*-thioxanthen-2-yl)carbonyl)oxy)methyl)-2,2-dimethyl-1,3-dioxolan-4-yl)methyl 7-methoxy-9-oxo-9H-thioxanthene-2-carboxylate [(*S,S*)-12]** Under a nitrogen atmosphere, substrate **11** (2.00 g, 6.99 mmol), ditosylate (*S,S*)-**4**[14] (1.10 g, 2.34 mmol), $K_2CO_3$ (1.06 g, 7.67 mmol), and $Bu_4NBr$ (250 mg, 0.78 mmol) were dissolved/suspended in DMF (50 mL). This suspension was heated to 90°C and stirred for 18h. After cooling, the DMF was evaporated under reduced pressure and the residue was dissolved in $CH_2Cl_2$. This suspension was filtered and the filtrate was concentrated *in vacuo* to yield a brown residue. Purification by column chromatography (silica gel, $CH_2Cl_2$/diethyl ether 20/1, $R_f$ = 0.24 for product) gave pure (*S,S*)-**12** (1.29 g, 1.85 mmol, 79%) as a yellow solid. $^1$H NMR (300 MHz, $CDCl_3$, 25°C) δ 9.12 (d, *J* = 2.1 Hz, 2H), 8.10 (dd, *J* = 8.4, 2.1 Hz 2H), 7.93, (d, *J* = 2.7 Hz, 2H), 7.49 (d, *J* = 8.4 Hz, 2H), 7.35 (d, *J* = 9.0 Hz, 2H), 7.18 (dd, *J* = 9.0, 2.7 Hz, 2H), 4.58 (m, 4H), 4.39 (s, 2H), 3.89 (s, 6H), 1.49 (s, 6H); $^{13}$C NMR (50 MHz, $CDCl_3$, 25°C) δ 178.61 (s), 165.18 (s), 158.64 (s), 158.64 (s), 142.46 (s), 131.68 (d), 129.97 (s), 128.03 (s), 128.03 (s), 127.28 (d), 127.19 (d), 126.19 (d), 122.86 (d), 110.48 (s), 109.41 (d), 76.26 (d), 64.64 (t), 55.65 (q), 27.13 (q); HRMS calcd for $C_{37}H_{30}O_{10}S_2$: 698.1280; found: 698.1283.

**(*S,S,M*)-5,33-Dimethoxy-19,19-dimethyl-15,18,20,23-tetraoxa-9,29-dithiaoctacyclo-[23.10.2.2$^{10,13}$.0$^{2,11}$.0$^{3,8}$.0$^{17,21}$.0$^{28,36}$.0$^{30,35}$]nonatriaconta-1,3,5,7,10(39),11,13(38),25,27,30,32,34,36-tridecaene-14,24-dione [(*S,S,M*)-13 (minor)]**

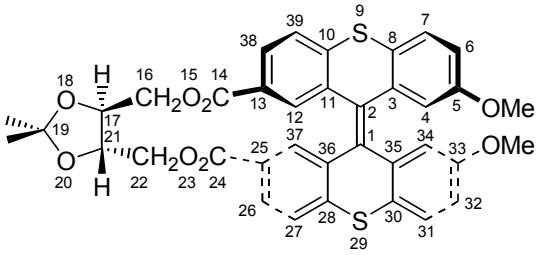


(*S,S,M*)-**13** (minor)

Under a nitrogen atmosphere, a solution of substrate (*S,S*)-**12** (744 mg, 1.07 mmol) in oxalyl dichloride (15 mL) was refluxed overnight. Excess of oxalyl dichloride was removed under reduced pressure and the residue was dissolved in freshly distilled *p*-xylene (30 mL, from sodium). Activated Cu-bronze[15] (520 mg, 8.18 mmol) was added and this suspension was refluxed for 24 h. After cooling, the mixture was filtered and the filtrate was concentrated *in vacuo* to yield a yellow residue. Purification by column chromatography (silica gel, $CH_2Cl_2$, $R_f$ = 0.30 for product) gave a mixture of two diastereoisomers (*S,S,P*)-**13** (major)/(*S,S,M*)-**13** (minor) 80/20 (142 mg, 0.21 mmol, 20%) as a yellow solid. Recrystallization from acetone afforded crystals of diastereomerically pure (*S,S,M*)-**13** (minor), suitable for X-ray analysis. $[\alpha]_D^{20}$ +203°, (c = 0.50, $CHCl_3$). $^1$H NMR (300 MHz, $CDCl_3$, 25°C) δ 7.65 (dd, *J* = 8.0, 1.8 Hz, $2H_{26,38}$), 7.53 (d, *J* = 8.0 Hz, $2H_{27,39}$), 7.37 (d, *J* = 8.6 Hz, $2H_{7,31}$), 7.08 (d, *J* = 1.8 Hz, $2H_{12,37}$), 6.77 (dd, *J* = 8.6, 2.3 Hz, $2H_{6,32}$), 6.35 (d, *J* = 2.3 Hz, $2H_{4,34}$), 4.29 (dd, *J* = 11.4, 6.4 Hz, $2H_{16,22,ax}$), 4.17 (d, *J* = 11.4 Hz, $2H_{16,22,eq}$), 3.98 (d, *J* = 6.4 Hz, $2H_{17,21}$), 3.38 (s, 6H, OMe), 1.56 (s, 6H, Me); $^{13}$C NMR (50 MHz, $CDCl_3$, 25°C) δ 165.55 (s), 158.24 (s), 141.86 (s), 136.09 (s), 133.11 (s), 133.40 (s), 130.78 (s), 127.52 (d), 127.47 (s), 127.33 (d), 126.40 (d), 125.25 (s), 115.52 (d), 114.02 (d), 108.51 (s), 79.77 (d), 63.83 (t), 55.19 (q), 26.53 (q); HRMS calcd for $C_{37}H_{30}O_8S_2$: 666.1382; found: 666.1394.

UV (*n*-hexane/*i*-propanol 80/20, λ (ε)): 205 nm (77900), 311 nm (17000)

CD (*n*-hexane/*i*-propanol 80/20, λ (Δε)): 221 nm (–44.2), 250 nm (+17.7), 273 nm (–6.2), 303 nm (+15.7), 341 nm (–2.4), 390 nm (+1.6)

**Crystal data of (*S,S,M*)-13 (minor)**

$C_{30}H_{37}O_8S_2$, monoclinic, space group $P2_1$, a = 9.598(1), b = 14.288(6), c = 12.383(3), Å, a = 9.598(1), b = 14.288(6), c = 12.383(3), V = 1587.8(8) $Å^3$, Z = 2, $D_x$ = 1.395 g $cm^{-3}$. X-ray data for a light yellow orange colored block shaped crystal, crystallized from acetone, were collected on an Enraf-Nonius CAD-4$F^2$ diffractometer, interfaced to a INDY (Silicon Graphics) UNIX computer (Mo tube, 50 kV, 40 mA, monochromated Mo-K$\bar{\alpha}$ radiation, $\Delta\varpi$ = 0.80 + 0.34 tg $\theta$. T = 130 K). Final refinement on $F^2$ carried out by full-matrix least-squares techniques converged at wR($F^2$) = 0.2108 for 2909 reflections with $F_o^2 \geq 0$ and $R(F)$ = 0.0701 for 2460 reflections with $F_o \geq 4.0\ \sigma(F_o)$ and 428 parameters.

**(*S,S,P*)-5,33-dimethoxy-19,19-dimethyl-15,18,20,23-tetraoxa-9,29-dithiaoctacyclo-[23.10.2.2$^{10,13}$.0$^{2,11}$.0$^{3,8}$.0$^{17,21}$.0$^{28,36}$.0$^{30,35}$]nonatriaconta-1,3,5,7,10(39),11,13(38),25,27,30,32,34,36-tridecaene-14,24-dione [(*S,S,P*)-13 (major)]**

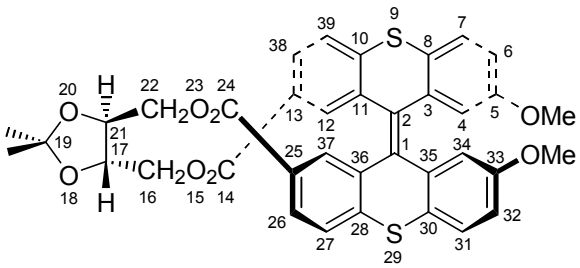


(*S,S,P*)-**13** (major)

See afore-mentioned procedure for (*S,S,M*)-**13** (minor). Despite several attempts the major isomer (*S,S,P*)-**13** could not be obtained in pure form. However, NMR-absorptions could be assigned. $^1$H NMR (300 MHz, $CDCl_3$, 25°C) δ 7.62 (dd, *J* = 8.1, 1.8 Hz, $2H_{26,38}$), 7.52 (d, *J* = 8.1 Hz, $2H_{27,39}$), 7.39 (d, *J* = 8.4 Hz, $2H_{7,31}$), 7.03 (d, *J* = 1.8 Hz, $2H_{12,37}$), 6.78 (dd, *J* = 8.4, 2.8 Hz, $2H_{6,32}$), 6.38 (d, *J* = 2.8 Hz, $2H_{4,34}$), 4.80 (dd, *J* = 11.7, 3.3 Hz, $2H_{16,22,eq}$), 4.29 (dd, *J* = 6.6, 3.3 Hz, $2H_{17,21}$), 4.02 (dd, *J* = 11.7, 6.6 Hz, $2H_{16,22,ax}$), 3.39 (s, 6H, OMe), 1.49 (s, 6H, Me); $^{13}$C NMR (50 MHz, $CDCl_3$, 25°C) δ 165.68 (s), 158.24 (s), 142.21 (s), 135.66 (s), 133.36 (s), 133.27 (s), 131.64 (d), 127.70 (d), 126.95 (s), 126.83 (d), 126.29 (d), 125.26 (s), 115.52 (d), 113.82 (d), 109.38 (s), 74.76 (d), 63.00 (t), 55.19 (q), 27.54 (q).

**(*R*)-1-(2-(((7-methoxy-9-oxo-9H-thioxanthen-2-yl)carbonyl)oxy)-1-naphthyl)-2-naphthyl 7-methoxy-9-oxo-9H-thioxanthene-2-carboxylate [(*R*)-14]** (same procedure holds for the (*S*)-**14** enantiomer). Substrate **11** (2.50 g, 8.74 mmol) was refluxed in $SOCl_2$ (25 mL) for 30 min. The excess of $SOCl_2$ was evaporated and the residue was stripped twice with benzene. The residue was dissolved in $CH_2Cl_2$ (25 mL) and the solution was added to a solution of (*R*)-binaphthol (*R*)-**3** (1.00 g, 3.49 mmol) and DMAP (40 mg) in $Et_3N$ (20 mL) and $CH_2Cl_2$ (20 mL). This mixture was stirred overnight at room temperature. The mixture was concentrated *in vacuo* and the residue was dissolved in $CH_2Cl_2$ (30 mL). After washing (twice with 2 M HCl (aq)) and drying ($Na_2SO_4$), the mixture was concentrated *in vacuo* to yield an orange residue. Purification by column chromatography ($Al_2O_3$ (6% water), $CH_2Cl_2$/*n*-hexane 5/1, $R_f$ = 0.75) gave pure (*R*)-**14** (2.70 g, 3.28 mmol, 94% based on (*R*)-binaphthol-**7**) as a yellow solid. $^1$H NMR (300 MHz, $CDCl_3$, 25°C) δ 9.02 (d, *J* = 1.8 Hz, 2H), 8.01 (d, *J* = 2.7 Hz, 2H), 7.96 (d, *J* = 9.0 Hz, 2H), 7.87 (d, *J* = 9.0 Hz, 2H), 7.76 (dd, *J* = 9.0, 1.8 Hz, 2H), 7.56 (d, *J* = 9.0 Hz, 2H), 7.35 – 7.46 (m, 10H), 7.23 (dd, *J* = 9.0, 2.7 Hz, 2H), 3.91 (s, 6H); $^{13}$C NMR (50 MHz, $CDCl_3$, 25°C) δ 178.41 (s), 163.88 (s), 158.51 (s), 146.97 (s), 142.47 (s), 133.32 (s), 131.95 (d), 131.66 (d), 131.61 (s), 129.87 (d), 129.82 (s), 128.08 (d), 127.89 (s), 127.81 (s), 127.17 (d), 127.00 (d), 126.82 (s), 126.13 (d), 126.06 (d), 125.88 (d), 123.68 (s), 122.61 (d), 121.73 (d), 110.32

(d), 55.45 (q); HRMS calcd for $C_{50}H_{30}O_8S_2$: 822.1382; found: 822.1399.

**(*R,P*)-5,46-dimethoxy-15,36-dioxa-9,42-dithiaundecacyclo [36.10.2.2$^{10,13}$.0$^{2,11}$.0$^{3,8}$.0$^{16,25}$.0$^{19,24}$.0$^{26,35}$.0$^{27,32}$.0$^{41,49}$.0$^{43,48}$]dopentaconta-1,3,5,7,10(52),11,13(51),16(25),17,19,21,23,26,28,30,32,34,38,40,43,45,47,49-tricosaene-14,37-dione [(*R,P*)-16 (major)]** (same procedure holds for (*R,M*)-**16** (minor), (*S,M*)-**16** (major), and (*S,P*)-**16** (minor)).

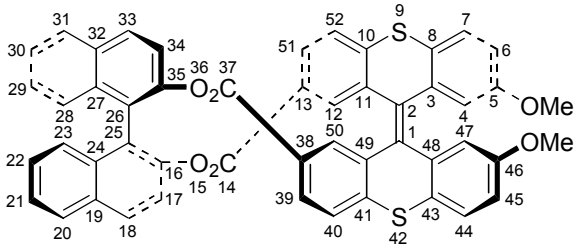


(*R,P*)-**16** (major)

Under a nitrogen atmosphere, substrate (*R*)-**14** (600 mg, 0.73 mmol) was refluxed overnight in oxalyl dichloride (20 mL). The excess of oxalyl dichloride was removed under reduced pressure. The residue was dissolved in freshly distilled *p*-xylene (100 mL, from sodium) and activated Cu-bronze[15] (1.01 g, 15.90 mmol) was added. This suspension was refluxed overnight. After cooling, the mixture was filtered and the filtrate was concentrated *in vacuo*. Purification of the residue by column chromatography (silica gel, $CH_2Cl_2$/*n*-hexane 3/1) gave 58 mg ($7.2 \times 10^{-2}$ mmol, 10%, $R_f$ = 0.26) of (*R,M*)-**16** (minor) and 254 mg (0.32 mmol, 44%, $R_f$ = 0.19) of (*R,P*)-**16** (major) as yellow solids. (*R,P*)-**16** (major): $[\alpha]_D^{20}$ –101° (c = 1.00, $CHCl_3$). (*S,M*)-**16** (major): $[\alpha]_D^{20}$ +100° (c = 1.00, $CHCl_3$). (*R,P*)-**16** (major) and (*S,M*)-**16** (major); $^1$H NMR (300 MHz, $CDCl_3$, 25°C) δ 7.96 (d, *J* = 8.8 Hz, $2H_{18,33}$), 7.91 (d, *J* = 8.4 Hz, $2H_{20,31}$), 7.42 (t, *J* = 8.4 Hz, $2H_{21,30}$), 7.38 (d, *J* = 8.8 Hz, $2H_{7,44}$), 7.36 (d, *J* = 8.4 Hz, $2H_{40,52}$), 7.31 (d, *J* = 1.5 Hz, $2H_{12,50}$), 7.25 (d, *J* = 8.8 Hz, $2H_{17,34}$), 7.25 (t, *J* = 8.4 Hz, $2H_{22,29}$), 7.11 (d, *J* = 8.4 Hz, $2H_{23,28}$), 7.01 (dd, *J* = 8.4, 1.5 Hz, $2H_{39,51}$), 6.74 (dd, *J* = 8.8, 2.6 Hz, $2H_{6,45}$), 6.36 (d, *J* = 2.6 Hz, $2H_{4,47}$), 3.39 (s, 6H, OMe); $^{13}$C NMR (75 MHz, $CDCl_3$, 25°C) δ 164.22 (s), 158.11 (s), 147.04 (s), 142.29 (s), 135.71 (s), 135.02 (s), 133.36 (s), 133.36 (s), 131.41 (s), 131.16 (d), 129.23 (d), 128.33 (d), 128.08 (d), 127.04 (d), 126.99 (s), 126.95 (d), 126.73 (d), 126.03 (s), 125.85 (d), 125.62 (d), 123.52 (s), 122.28 (d), 115.20 (d), 113.66 (d), 55.10 (q); HRMS calcd for $C_{50}H_{30}O_6S_2$: 790.1484; found: 790.1494.

UV (*n*-hexane/*i*-propanol 80/20, λ (ε)): 224 nm (125000), 278 nm (25600), 306 nm (21400)

CD (*S,M*)-**16** (major): (*n*-hexane/*i*-propanol 80/20, λ (Δε)): 212 nm (+53.4), 224 nm (+110.9), 234 nm (–39.3), 242 nm (+8.9), 257 nm (–33.2), 293 nm (+6.6), 313 nm (–24.7)

**(*R,P*)-5,46-dimethoxy-15,36-dioxa-9,42-dithiaundecacyclo [36.10.2.2$^{10,13}$.0$^{2,11}$.0$^{3,8}$.0$^{16,25}$.0$^{19,24}$.0$^{26,35}$.0$^{27,32}$.0$^{41,49}$.0$^{43,48}$]dopentaconta-1,3,5,7,10(52),11,13(51),16,18,20,22,24,26(35),27,29,31,33,38,40,43,45,47,49-tricosaene-14,37-dione [(*R,M*)-16 (minor)]** (*R,M*)-**16** (minor): $[\alpha]_D^{20}$ +120° (c = 1.00, $CHCl_3$). (*S,P*)-**16** (minor): $[\alpha]_D^{20}$ –120° (c = 1.00, $CHCl_3$). (*R,M*)-**16** (minor) and (*S,P*)-**16** (minor); $^1$H NMR (300 MHz, $CDCl_3$, 25°C) δ 8.00 (d, *J* = 9.5 Hz, $2H_{18,33}$), 7.95 (d, *J* = 8.4 Hz, $2H_{20,31}$), 7.54 (d, *J* = 1.5 Hz, $2H_{12,50}$), 7.48 (t, *J* = 8.4 Hz, $2H_{21,30}$), 7.46 (d, *J* = 8.4 Hz, $2H_{40,52}$), 7.40 (d, *J* = 8.4 Hz, $2H_{7,44}$), 7.39 (d, *J* = 9.5 Hz, $2H_{17,34}$), 7.39 (dd, *J* = 8.4, 1.5 Hz, $2H_{39,51}$), 7.24 (t, *J* = 8.4 Hz, $2H_{22,29}$), 7.07 (d, *J* = 8.4 Hz, $2H_{23,28}$), 6.79 (dd, *J* = 8.4, 2.9 Hz, $2H_{6,45}$), 6.39 (d, *J* = 2.9 Hz, $2H_{4,47}$), 3.39 (s, 6H, OMe); $^{13}$C NMR (50 MHz, $CDCl_3$, 25°C) δ 165.26 (s), 158.40 (s), 146.92 (s), 141.66 (s), 136.54 (s), 134.16 (s), 133.50 (s), 132.98 (s), 131.70 (s), 131.20 (d), 129.67 (d), 128.03 (d), 127.81 (s), 127.61

(d), 127.49 (d), 127.17 (d), 126.99 (d), 126.59 (d), 125.67 (d), 125.39 (s), 123.25 (s), 122.47 (d), 115.71 (d), 114.52 (d), 55.18 (q); HRMS calcd for $C_{50}H_{30}O_6S_2$: 790.1484; found: 790.1494.

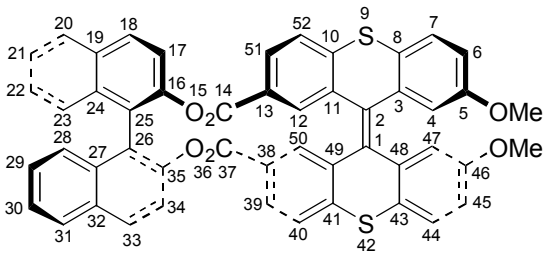


(*R,M*)-**16** (minor)

UV (*n*-hexane/*i*-propanol 80/20, λ (ε)): 222 nm (148600), 286 nm (30400), 378 nm (7100)

CD (*R,M*)-**16** (minor): (*n*-hexane/*i*-propanol 80/20, λ (Δε)): 216 nm (+95.8), 225 nm (–264.0), 236 nm (+86.3), 251 nm (–37.9), 276 nm (+3.7), 293 nm (–24.9), 318 nm (+41.1)

**(9-(2-(hydroxymethyl)-7-methoxy-9H-thioxanthen-9-ylidene)-7-methoxy-9H-thioxanthen-2-yl)-methanol [*cis*-17]** General procedure for cleavage of the chiral template from overcrowded alkenes **13** and **16** to yield *cis*-**17**. Under a nitrogen atmosphere, $LiAlH_4$ (~ 0.30 mmol) was suspended in diethyl ether (2.0 mL) at 0°C. The overcrowded alkene [(*S,S,M*)-**13** (minor), (*R,P*)-**16** (major), (*R,M*)-**16** (minor), (*S,M*)-**16** (major), or (*S,P*)-**16** (minor), ~3.5 × $10^{-2}$ mmol] was added and the reaction mixture was stirred for 3 h at 5°C. The diethyl ether was removed under reduced pressure at room temperature and the residue was dissolved in $CH_2Cl_2$ (10 mL) and 2 M HCl (aq) (10 mL) (all liquids were cooled to 0°C before used during workup to avoid racemization of *cis*-**17**). The organic and water layer were separated and the organic layer was washed (1 × 10 mL of 2 M HCl (aq)), dried ($Na_2SO_4$), and concentrated *in vacuo* to yield a yellowish powder. The powder was dissolved (binaphthol) and suspended (*cis*-**17**) in a mixture of *n*-hexane/$CH_2Cl_2$ 1/1 (4.0 mL) and stirred for 15 min. Diol *cis*-**17** was collected on a glass filter in 90 – 95% yield as a slightly yellow powder. $^1$H NMR (300 MHz, DMSO-$d_6$, 25°C) δ 7.56 (d, $J$ = 8.4 Hz, 2H), 7.53 (d, $J$ = 8.8 Hz, 2H), 7.17 (dd, $J$ = 8.4, 1.3 Hz 2H), 6.85 (dd, $J$ = 7.0, 2.6 Hz, 2H), 6.60 (d, $J$ = 1.3 Hz, 2H), 6.24 (d, $J$ = 2.6 Hz, 2H), 5.02 (t, $J$ = 5.3 Hz, 2H), 4.11 (d, $J$ = 5.3 Hz, 4H), 3.35 (s, 6H); $^{13}$C NMR (50 MHz, DMSO-$d_6$, 25°C) δ 157.57 (s), 140.19 (s), 135.39 (s), 133.41 (s), 133.14 (s), 133.02 (s), 128.04 (d), 127.49 (d), 126.74 (d), 126.00 (s), 125.51 (d), 114.72 (d), 113.88 (d), 62.17 (t), 54.89 (q); HRMS calcd for $C_{30}H_{24}O_4S_2$: 512.1116; found: 512.1102.

| | | |
|---|---|---|
| (*M*)-*cis*-**17** from (*S,S,M*)-**13** (minor): | $[\alpha]_D^{20}$ | –92° (c = 1.00, $CHCl_3$) |
| (*P*)-*cis*-**17** from (*R,P*)-**16** (major): | $[\alpha]_D^{20}$ | +91° (c = 1.00, $CHCl_3$) |
| (*M*)-*cis*-**17** from (*R,M*)-**16** (minor): | $[\alpha]_D^{20}$ | –93° (c = 1.00, $CHCl_3$) |
| (*M*)-*cis*-**17** from (*S,M*)-**16** (major): | $[\alpha]_D^{20}$ | –92° (c = 1.00, $CHCl_3$) |
| (*P*)-*cis*-**17** from (*S,P*)-**16** (minor): | $[\alpha]_D^{20}$ | +91° (c = 1.00, $CHCl_3$) |

UV (*n*-hexane/*i*-propanol 80/20, λ (ε)): 214 nm (67000), 272 nm (15800), 372 nm (6200)

CD (*P*)-*cis*-**17**: (*n*-hexane/*i*-propanol 80/20, λ (Δε)): 220 nm (+37.9) 229 nm (–17.6) 239 nm (+11.6), 252 nm (–18.0), 270 nm (+22.6), 291 nm (–46.8), 313 nm (+17.5)

Determination of $\Delta G^{\ddagger}_{rac.}$ of compound *cis*-**17** (polarimetry, dibromoethane, 589 nm):
k = 7.22 × $10^{-5}$ $s^{-1}$ at 70.0°C, $\Delta G^{\ddagger}$ = 26.7 kcal $mol^{-1}$

The e.e. values of (*P*)-*cis*-**17** and (*M*)-*cis*-**17** were determined by chiral HPLC (Daicel, chiralcel OD column, flow rate 1.0 mL $min^{-1}$, *n*-hexane/*i*-propanol, 99/1): $t_{ret.}$ 98 min for (*P*)-*cis*-**17** and $t_{ret.}$ 125 min for (*M*)-*cis*-**17**.

## 2.8 References


1 Part of this chapter has been published: E. M. Geertsema, A. Meetsma, B. L. Feringa, *Angew. Chem. Int.* **1999**, *38*, 2738.

2 a) W. T. Grubb, G. B. Kistiakowsky, *J. Am. Chem. Soc.* **1950**, *72*, 419; b) J. H. Day, *Chem. Rev*. **1963**, *63*, 65; c) J. Sandström, *Top. Stereochem*. (Eds.: N. L. Allinger, E. L. Eliel, S. H. Wilen), Wiley, New York, **1983**, *14*, 83; d) G. Shoham, S. Cohen, R. M. Suissa, I. Agranat in *Molecular Structure: Chemical Reactivity and Biological Activity* (Eds.: J. J. Stezowsky, J.-L. Huang, M.-C. Shao), IUCR Crystallographic Symposia 2, Oxford University Press, Oxford, **1988**, 290; e) 'Photochromism, Molecules and Systems' in *studies in Organic Chemistry 40* (eds.: H. Dürr, H. Bouas Laurent), Elsevier, Amsterdam, **1990**; f) W. Luef, R. Keese, *Top. Stereochem*. **1991**, *20*, 231; g) J. Sandström in: *The chemistry of double-bonded functional groups*, *Supplement A3*, (ed.: S. Patai), Wiley, New York, **1997**, 1253; h) P. U. Biedermann, J. J. Stezowski, I. Agranat, in: *Advances in Theoretically Interesting Molecules*, vol. 4 (Ed.: R. P. Thummel), JAI Press, Stamford, Connecticut, **1998**, 245; i) P. U. Biedermann, J. J. Stezowsky, I. Agranat, *Eur. J. Org. Chem*. **2001**, 15; j) A. Z.-Q. Khan, J. Sandström, *J. Am. Chem. Soc.*, **1988**, *110*, 4843.

3 a) B. L. Feringa, W. F. Jager, B. de Lange, *Tetrahedron* **1993**, *49*, 8267; b) B. L. Feringa, N. P. M. Huck, A. M. Schoevaars, *Adv. Mater*. **1996**, *8*, 681; c) W. F. Jager, J. C. de Jong, B. de Lange, N. P. M. Huck, A. Meetsma, B. L. Feringa, *Angew. Chem. Int.* **1995**, *34*, 348; d) B. L. Feringa, R. A. van Delden, N. Koumura, E. M. Geertsema, *Chem. Rev*. **2000**, *100*, 1789; e) Special issue on Photochromism: Memories and Switches, *Chem. Rev*. **2000**, *100*; f) B. L. Feringa (ed.), Molecular Switches, Wiley-VCH, Darmstadt, **2001**.

4 a) B. L. Feringa, N. P. M. Huck, H. A. van Doren, *J. Am. Chem. Soc*. **1995**, *117*, 9929; b) N. P. M. Huck, W. F. Jager, B. de Lange, B. L. Feringa, *Science* **1996**, *273*, 1686.

5 M. L. C. M. Oosterling, A. M. Schoevaars, H. J. Haitjema, B. L. Feringa, *Isr. J. Chem*. **1996**, *36*, 341.

6 a) S. Miyano, H. Fukushima, S. Handa, H. Ito, H. Hashimoto, *Bull. Chem. Soc. Jpn*. **1988**, *61*, 3249 and references therein; b) B. H. Lipshutz, Z. Liu, F. Kayser, *Tetrahedron Lett*. **1994**, *35*, 5567; c) M. Tanaka, H. Mitsuhashi, M. Maruno, T. Wakamatsu, *Tetrahedron Lett*. **1994**, *35*, 3733; d) V. H. Rawal, A. S. Florjancic, S. P. Singh, *Tetrahedron Lett*. **1994**, *35*, 8985; e) K. S. Feldman, A. Sambandam, *J. Org. Chem*. **1995**, *60*, 8171.

7 T. Sugimura, H. Yamada, S. Inoue, A. Tai, *Tetrahedron: Asymmetry* **1997**, *8*, 649.

8 a) Y. C. Yip, X. Wang, D. K. P. Ng, T. C. W. Mak, P. Chiang, T. Luh, *J. Org. Chem*. **1990**, *55*, 1881; b) X. Wang, T. Luh, *J. Org. Chem*. **1989**, *54*, 263.

9 W. F. Jager, Chiroptical Molecular Switches, *Application of inherently dissymmetric alkenes*. Ph.D. Thesis, Groningen, **1994**.

10 a) A. Schönberg, S. Nickel, *Ber*. **1934**, *67*, 1795; b) A. Schönberg, W. Asker, *J. Chem. Soc*. **1942**, 272; c) A. Schönberg, A. Mustafa, M. E. El-Din Sobhy, *J. Am. Chem. Soc*. **1953**, *75*, 3377; d) A. Mustafa, M. E. El-Din Sobhy, *J. Am. Chem. Soc*. **1955**, *77*, 5124; e) A. Mustafa, W. Asker, M. E. El-Din Sobhy, *J. Org. Chem*. **1960**, *25*, 1519.

11 K. Nozaki, T. Terakawa, H. Takaya, T. Hiyama, *Angew. Chem. Int.* **1998**, *37*, 131.

12 The model of (*R,P*)-**16** (major) was constructed by using Quanta97/CHARMm (a product of Molecular Simulations Inc., San Diego, USA).

13 W. F. Jager, B. de Lange, A. M. Schoevaars, F. van Bolhuis, B. L. Feringa, *Tetrahedron: Asymmetry* **1993**, *4*, 1481.

14 J. M. Townsend, J. F. Blount, R. Chu Sun, S. Zawoiski, D. Valentine jr., *J. Org. Chem.* **1980**, *45*, 2995.

15 B. S. Furniss, A. J. Hannaford, V. Rogers, P. W. G. Smith, A. R. Tatchell, *Vogel's Textbook of Practical Organic Chemistry*, Longman, London and New York, *Fourth edition*, **1978**, pages 285 and 611.